The EMBO Journal (2008) 27, 1299–1308 | © 2008 European Molecular Biology Organization | All Rights Reserved 0261-4189/08
www.embojournal.org

THE EMBO JOURNAL

Mechanism of intercellular molecular exchange in heterocyst-forming cyanobacteria

Conrad W Mullineaux[1,*], Vicente Mariscal[2], Anja Nenninger[1], Hajara Khanum[1], Antonia Herrero[2], Enrique Flores[2] and David G Adams[3]

[1]School of Biological and Chemical Sciences, Queen Mary, University of London, London, UK, [2]Instituto de Bioquímica Vegetal y Fotosíntesis, CSIC, Universidad de Sevilla, Sevilla, Spain and [3]Faculty of Biological Sciences, Institute of Integrative and Comparative Biology, University of Leeds, Leeds, UK

Heterocyst-forming filamentous cyanobacteria are true multicellular prokaryotes, in which heterocysts and vegetative cells have complementary metabolism and are mutually dependent. The mechanism for metabolite exchange between cells has remained unclear. To gain insight into the mechanism and kinetics of metabolite exchange, we introduced calcein, a 623-Da fluorophore, into the *Anabaena* cytoplasm. We used fluorescence recovery after photobleaching to quantify rapid diffusion of this molecule between the cytoplasms of all the cells in the filament. This indicates nonspecific intercellular channels allowing the movement of molecules from cytoplasm to cytoplasm. We quantify rates of molecular exchange as filaments adapt to diazotrophic growth. Exchange among vegetative cells becomes faster as filaments differentiate, becoming considerably faster than exchange with heterocysts. Slower exchange is probably a price paid to maintain a microaerobic environment in the heterocyst. We show that the slower exchange is partly due to the presence of cyanophycin polar nodules in heterocysts. The phenotype of a null mutant identifies FraG (SepJ), a membrane protein localised at the cell–cell interface, as a strong candidate for the channel-forming protein.

The EMBO Journal (2008) **27,** 1299–1308. doi:10.1038/emboj.2008.66; Published online 3 April 2008
Subject Categories: membranes & transport; plant biology
Keywords: *Anabaena*; cell communication; cyanobacterium; heterocyst; microplasmodesmata

Introduction

Filamentous cyanobacteria such as *Anabaena cylindrica* and related species are true multicellular prokaryotes. Filaments consist of linear chains of cells that, depending on growth conditions, may contain two or more cooperating cell types (Golden and Yoon, 2003). When cells are deprived of combined nitrogen compounds, approximately one cell in ten differentiates to form a nitrogen-fixing heterocyst. The other cells remain as vegetative cells, carrying out oxygenic photosynthesis and fixing carbon dioxide. Heterocysts and vegetative cells are mutually dependent, with the vegetative cells supplying sugars and heterocysts supplying combined nitrogen compounds (Golden and Yoon, 2003). The heterocysts are evenly spaced along the filament: a simple paradigm for biological pattern formation (Wolk, 1991; Zhang *et al*, 2006; Xu *et al*, 2008). Key steps in the evolution of this form of prokaryotic multicellularity must have included the development of intercellular signalling mechanisms, and efficient mechanisms for metabolite exchange between cells. Despite intensive study of the genetics and physiology of heterocyst differentiation, these cell communication mechanisms have remained unclear (Zhang *et al*, 2006). Ultrastructural studies suggest the possibility of interconnecting structures (termed 'microplasmodesmata') that may form channels linking the cytoplasms of adjacent cells (Giddings and Staehelin, 1978, 1981). These structures appear as pits or protuberances in freeze-fracture electron micrographs (Giddings and Staehelin, 1978). In thin-section electron micrographs, they sometimes appear as thin strands of electron-dense stained material perpendicular to the septum wall and apparently linking the plasma membranes of the two cells (Giddings and Staehelin, 1978). The structures may bear some resemblance to the gap junctions of animal cells (Söhl *et al*, 2005). However, BLAST searches of the sequenced cyanobacterial genomes reveal no homologs of the gap junction protein connexin, indicating that the animal and cyanobacterial systems have no evolutionary relationship. A clear difference between gap junctions and the putative intercellular connections in cyanobacteria is that in gap junctions the plasma membranes of the two connected cells are brought very close together (Söhl *et al*, 2005). By contrast, a cyanobacterial connection would have to span a significant gap of perhaps 30–40 nm between the two plasma membranes, and would have to traverse two cell walls (Giddings and Staehelin, 1978). Another possible model would be the plasmodesmata of plants (Lucas and Lee, 2004). However, these are wider structures lined with plasma membrane, and electron microscopy provides no indication of such structures in cyanobacteria (Flores *et al*, 2006). The 'microplasmodesmata' observed by freeze-fracture electron microscopy have an external diameter of only 20 nm (Giddings and Staehelin, 1978) and are therefore much more likely to be channels formed by protein oligomers (Flores *et al*, 2006).

There has never been a clear functional demonstration of cytoplasmic connections in a prokaryote. An alternative interpretation for the interconnecting structures seen in *Anabaena* is that they simply have an anchoring role, with molecular exchange instead occurring through a continuous periplasm (Flores *et al*, 2006).

Here, we directly visualise molecular exchange between cells in several *Anabaena* species by loading calcein, a small

*Corresponding author. School of Biological and Chemical Sciences, Queen Mary, University of London, Mile End Road, London E1 4NS, UK. Tel.: +44 20 7882 7008; Fax: +44 20 8983 0973;
E-mail: c.mullineaux@qmul.ac.uk

Received: 13 December 2007; accepted: 4 March 2008; published online: 3 April 2008

hydrophilic fluorophore, into the cytoplasm. We use fluorescence recovery after photobleaching (FRAP) to observe and quantify rapid diffusion of calcein between the cytoplasms of all the cells in the filament. Studies on two *Anabaena* mutants provide insight into the molecular machinery involved, and the factors that control rates of molecular exchange between cells.

Results and discussion

Calcein can be loaded into the cytoplasm of filamentous cyanobacteria

We set out to visualise intercellular molecular exchange by FRAP, using a laser-scanning confocal microscope. The first requirement is to place a hydrophilic fluorescent molecule in the cytoplasm. It is already clear that cytoplasmic green fluorescent protein (GFP) cannot exchange between heterocysts and vegetative cells. GFP expressed in vegetative cells of *Anabaena* sp. PCC7120 does not spread to heterocysts (Yoon and Golden, 1998), and vice versa (Mariscal *et al*, 2007). However, there may be pores that allow the exchange of smaller molecules. The fluorescein derivative calcein is available as a non-fluorescent acetoxymethylester (AM) derivative, which is sufficiently hydrophobic to traverse cell membranes. In the cytoplasm, the ester groups are hydrolysed by endogenous esterases to produce a fluorescent, hydrophilic product of 623 Da (Haugland, 2005). Unlike some related cytoplasmic tracers such as CellTracker™, calcein has no thiol-reactive groups and therefore no tendency to combine with proteins or glutathione (Haugland, 2005). We found that calcein-AM can readily be loaded into cells of filamentous cyanobacteria including *A. cylindrica* (Figure 1). The green fluorescence of calcein can easily be distinguished from the red fluorescence from chlorophyll in the intracellular thylakoid membranes. Chlorophyll fluorescence can be used as a reference for the location of other fluorophores in cyanobacterial cells (Spence *et al*, 2003; Komenda *et al*, 2006). For example, GFP in the periplasm shows as a green fluorescent 'halo' outside the chlorophyll fluorescence (Spence *et al*, 2003; Mariscal *et al*, 2007). Chlorophyll fluorescence also provides a good way of recognising heterocysts, as heterocysts have much lower chlorophyll fluorescence than vegetative cells (Zhang *et al*, 2006). Figure 1 compares the distribution of calcein fluorescence, chlorophyll fluorescence and fluorescence from BODIPY® FL C_{12}, a lipophilic green fluorophore (Sarcina *et al*, 2003; Haugland, 2005) that stains the outer layers of the cells (Figure 1B and D). These images were recorded using a tight confocal pinhole to give a *Z*-resolution much smaller than the diameter of the cell. Thus, we are taking an optical section through the mid-plane of the cell. This ensures that the effective optical path length is similar, regardless of position in the cell, allowing us to assess the relative concentrations of the dye in different regions of the cell. Unstained cells imaged with the same settings showed negligible green fluorescence (not shown). Calcein is located in the cytoplasm, with no detectable calcein fluorescence in the periplasm (Figure 1A and C). In filaments grown in the absence of combined nitrogen to induce heterocyst formation, calcein is loaded into the cytoplasm of heterocysts as well as vegetative cells (Figure 1C). All measurements were carried out on cells that had been washed and incubated in dye-free medium for at least 90 min. Calcein fluorescence was retained, confirming that the dye is trapped in the cytoplasm. We monitored calcein fluorescence for several minutes and found that it was stable (not shown), confirming that production of the fluorescent dye by ester hydrolysis was complete.

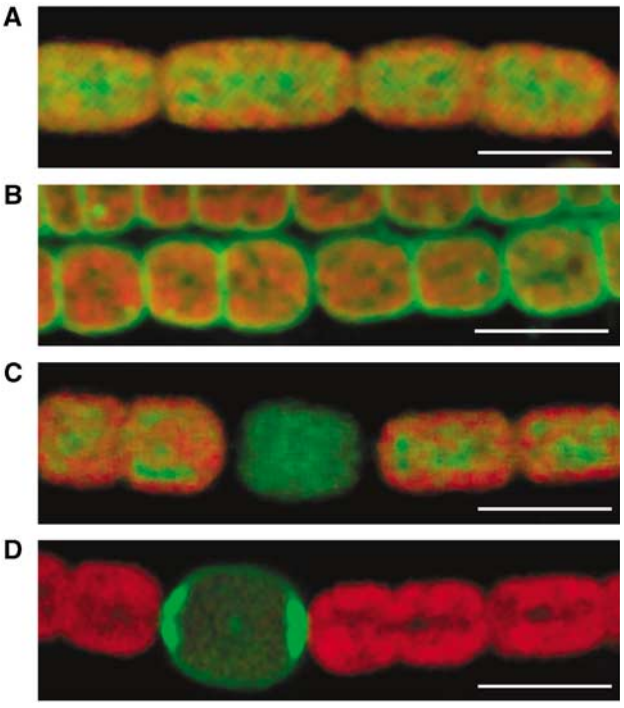

Figure 1 Distribution of fluorescent dyes in filaments of *Anabaena cylindrica*. Fluorescence micrographs with excitation at 488 nm. Resolution in the *Z*-direction was 1.3 μm (full width at half-maximum of the point spread function). Chlorophyll fluorescence (>665 nm) is shown in red, and green dye fluorescence (500–527 nm) is shown in green. All scale bars 10 μm. (**A**) An undifferentiated (nitrate-grown) filament stained with calcein. (**B**) An undifferentiated filament stained with BODIPY® FL C_{12}. (**C**) A differentiated filament stained with calcein. The cell with low chlorophyll fluorescence is a heterocyst. (**D**) A differentiated filament stained with BODIPY® FL C_{12}. The green fluorescent cell is a heterocyst. In contrast to undifferentiated filaments (B), BODIPY® FL C_{12} does not stain vegetative cells under these conditions.

Rapid exchange of calcein between the cytoplasms of vegetative cells

Having established that calcein can be loaded into the cytoplasm in filamentous cyanobacteria, we used FRAP measurements to probe the ability of calcein to diffuse from cell to cell. For these measurements, we used a lower *Z*-resolution to give a more complete measurement of cytoplasmic dye concentration. The principle of the measurement is that the focused laser spot of the laser-scanning confocal microscope can be used to bleach calcein fluorescence in a single cell in the filament. If the calcein cannot diffuse from cell to cell, fluorescence in that cell should remain bleached. If intercellular diffusion is possible, fluorescence in the bleached cell will recover, accompanied by a decrease in fluorescence in the neighbouring cells. The kinetics of the fluorescence changes will indicate the kinetics of molecular exchange. An important control is to check that the photochemical bleaching is irreversible: that is, the fluorescence of bleached calcein does not spontaneously recover. We bleached

fluorescence in isolated cells and entire short filaments of *Anabaena* grown under a variety of conditions, and in no case did we see any fluorescence recovery on the 1–2 min timescale of our measurements, either in vegetative cells or heterocysts (not shown). Therefore, we can be confident that bleaching is irreversible, and, where fluorescence recovery is seen, it is due to diffusion.

Filaments of *A. cylindrica* grown with nitrate consist of long chains of vegetative cells. A typical FRAP measurement on such a filament is shown in Figure 2. Diffusion of calcein within the cytoplasm of the bleached cell is so rapid that we could not resolve it: the calcein completely re-equilibrates within the cytoplasm during the 1–2 s bleaching time. This is not surprising in view of the very rapid diffusion of molecules in the bacterial cytoplasm (Mullineaux *et al*, 2006). Before the first post-bleach image can be recorded, the bleach also spreads into neighbouring cells, providing a first indication of rapid calcein exchange between vegetative cells (Figure 2A). Over the next few seconds there is further equilibration of calcein fluorescence among the cells in the filament, resulting in fluorescence recovery in the bleached cell (Figure 2A and B). The changes are clearly due to redistribution of calcein, as fluorescence recovery in the bleached cell is accompanied by loss of fluorescence elsewhere in the filament, most noticeable in the terminal cell at the top of the picture (Figure 2A and B). The changes seen show all the hallmarks of random diffusion, with calcein fluorescence simply flowing down the concentration gradient created by the bleach. There is no indication of the directionality imposed by active transport.

Quantification of the kinetics of intercellular exchange

The diffusion of calcein from cell to cell (seen in Figure 2 for example) differs from 'classical' diffusion in that it is not spatially homogeneous. Our FRAP measurements show that diffusion within the cytoplasm of an individual cell is too rapid for us to quantify in our experimental set-up. We were unable to detect concentration gradients within the cytoplasm, indicating that the dye always re-equilibrates during the time required to carry out the bleach and record the first image. However, there are clear barriers to diffusion between cells, leading to stepwise differences in dye concentration between neighbouring cells (e.g. Figure 2B). This shows that the rate-limiting step in the spread of calcein along the filament is movement across the cell–cell interface. Therefore, we quantified the kinetics of dye exchange between cells in terms of an 'exchange coefficient' (E), which relates the observed rate of dye movement between two neighbouring cells to the difference in dye concentration between the two cells. For pairwise exchange of dye between two neighbouring cells

$$\text{Net rate of exchange from cell 1 to cell 2} = E(C_1 - C_2) \quad (1)$$

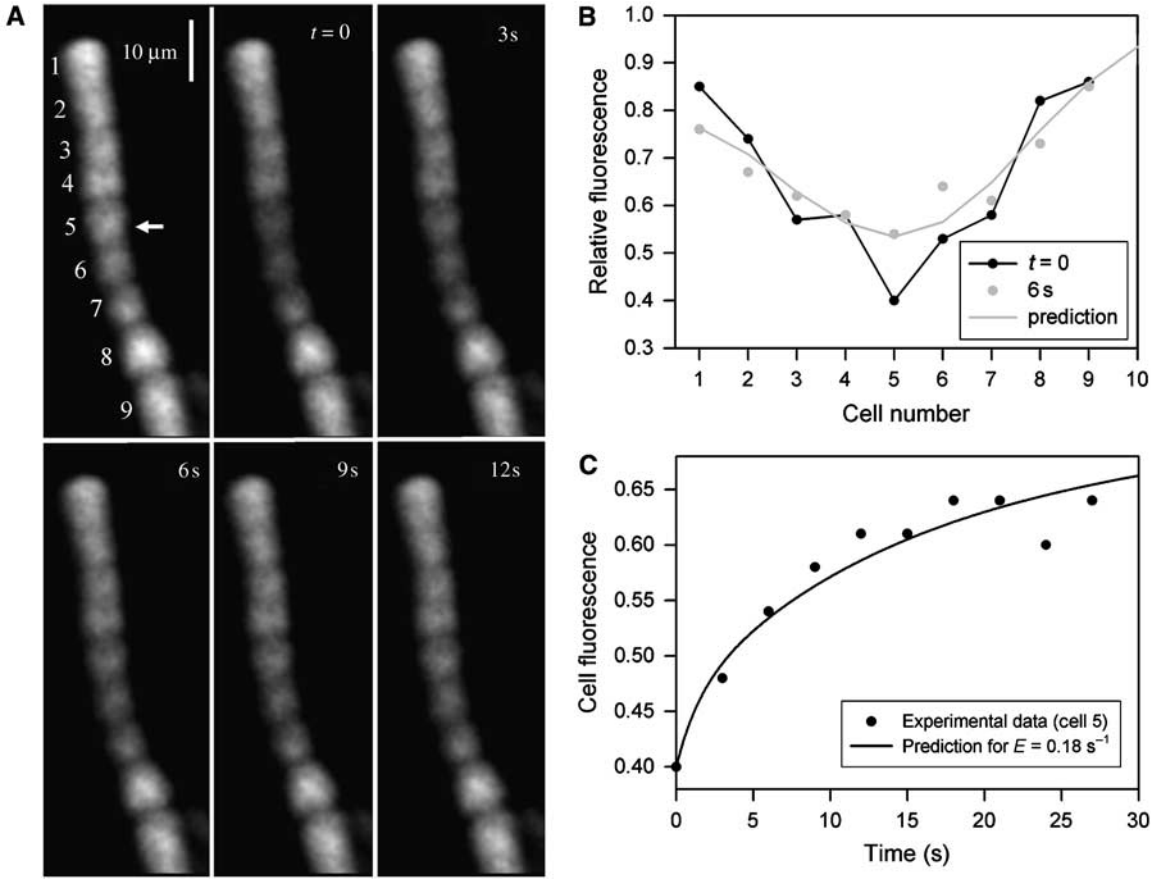

Figure 2 Calcein FRAP measurement in vegetative cells of *Anabaena cylindrica* (cells grown with nitrate). (**A**) FRAP image sequence. Only calcein fluorescence is shown. The image at top left was recorded prior to bleaching; the arrow indicates the position of the line bleach and the cell numbers used in (B) and (C) are indicated. (**B**) Quantitation of cell fluorescence in the FRAP sequence shown in (A). Total fluorescence from each cell is expressed relative to fluorescence from the same cell prior to the bleach. Data are for $t = 0$ and 6 s, with the predicted fluorescence levels at 6 s, for $E = 0.18\,s^{-1}$. (**C**). Fluorescence recovery of cell 5, fit to the predicted recovery curve for $E = 0.18\,s^{-1}$.

Table I Cell–cell exchange coefficients for calcein in filaments of *Anabaena cylindrica*

Measurement	Mean exchange coefficient (s^{-1}) ($\pm$s.d.)
1. Vegetative cells in nitrate-grown filaments	0.11 ± 0.03
2. Vegetative cells after 18 h of nitrate deprivation	0.14 ± 0.05
3. Vegetative cells to pro-heterocysts after 18 h of nitrate deprivation	0.034 ± 0.011
4. Vegetative cells after 72 h of nitrate deprivation	0.29 ± 0.13
5. Vegetative cells to heterocysts after 72 h of nitrate deprivation	0.022 ± 0.011

t-Tests indicate that E is significantly different in (1) and (3) ($P = 0.0001$); (2) and (4) ($P = 0.02$); (2) and (3) ($P = 0.0003$); (4) and (5) ($P = 0.0002$).

where C_n is the concentration of dye in cell n and E is the exchange coefficient. In an extended filament, analytical solutions become difficult but molecular redistribution can be predicted by an iterative model in which the incremental change in dye concentration in any cell (δC_n) within a time increment δt is determined by the instantaneous concentration differences with its two neighbours

$$\begin{aligned} \delta C_n &= E\delta t\{(C_{n+1} - C_n) + (C_{n-1} - C_n)\} \\ &= E\delta t(C_{n+1} + C_{n-1} - 2C_n) \end{aligned} \quad (2)$$

For an undifferentiated filament such as that shown in Figure 2, it is reasonable to make the simplifying assumption that E is the same for every cell junction in the filament. We can then take the fluorescence pattern seen in the first image after the bleach (Figure 2B) and use an iterative routine to predict how it will evolve with time, for a given value for E. The actual value for E can be obtained by fitting the predicted recovery curve for the bleached cell onto the experimentally obtained recovery curve (Figure 2C). This procedure gives an estimated E of $0.18\ s^{-1}$ for the filament shown in Figure 2. We found significant variation from filament to filament, with a mean E-value under these conditions of $0.11 \pm 0.03\ s^{-1}$ (Table I). Note that our model gives a good prediction for the kinetics of recovery in the bleached cell (Figure 2C) and also for the fluorescence changes observed in neighbouring cells (Figure 2B).

Calcein exchange between heterocysts and vegetative cells

We next looked at *A. cylindrica* filaments in which heterocyst development had been induced by growth in the absence of combined nitrogen for 72 h. Dye exchange between vegetative cells was observed using FRAP measurements in which one cell within an extended sequence of vegetative cells was bleached. Once again we observed rapid exchange of dye between vegetative cells (not shown). We quantified exchange among vegetative cells as described above and found that it becomes significantly faster after heterocyst differentiation (Table I). This suggests an increase in the number or activity of connections between vegetative cells.

Dye exchange between heterocysts and vegetative cells was observed by bleaching fluorescence in the heterocyst cytoplasm (Figure 3A). Fluorescence recovery occurs, but on a slower timescale than with vegetative cells (Figure 3A). Fluorescence remained approximately constant in the neighbouring vegetative cells, indicating that the dye re-equilibrated among the vegetative cells much faster than it exchanged with the heterocyst (Figure 3A).

The junctions between heterocysts and vegetative cells are asymmetric. Therefore, we considered the possibility that the exchange coefficients might be different for influx (E_{in}) and efflux of dye from the heterocyst (E_{out}). We used filaments washed in dye-free medium for at least 90 min. Therefore, there is ample time for equilibration of the dye in the filament. At equilibrium, the rates of dye efflux and influx must be the same, therefore

$$C_H E_{out} = C_V E_{in} \text{ and thus } C_V/C_H = E_{out}/E_{in} \quad (3)$$

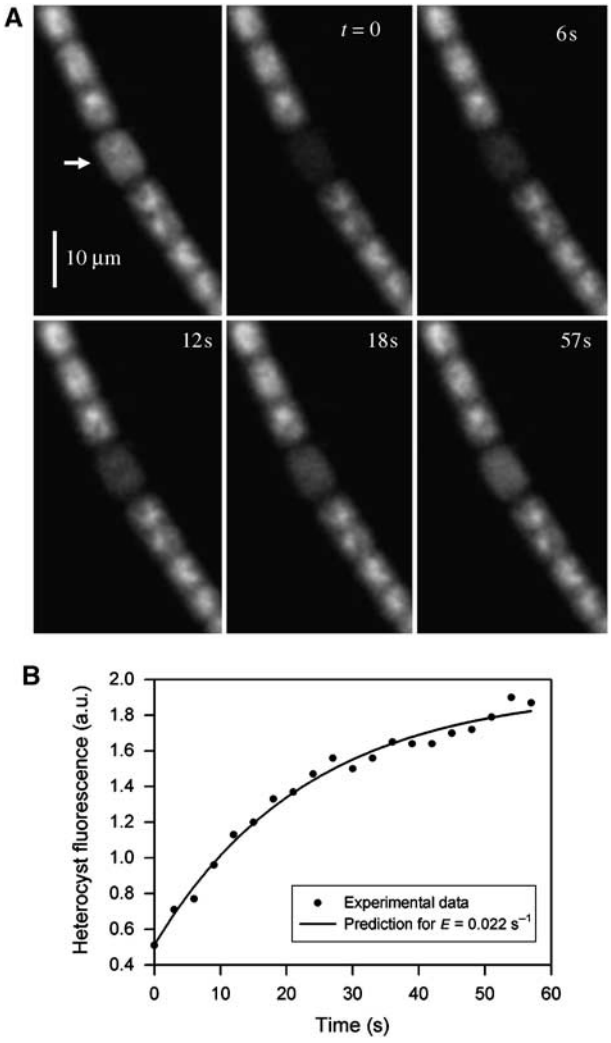

Figure 3 Calcein FRAP measurement in a heterocyst of *Anabaena cylindrica*. (**A**) FRAP image sequence showing calcein fluorescence. The image at top left was recorded prior to bleaching the heterocyst; the arrow indicates the position of the line bleach. (**B**) Fluorescence recovery of the heterocyst, fit to the predicted recovery curve for $E = 0.022\ s^{-1}$.

where C_H is the dye concentration in the heterocyst and C_V is the dye concentration in the neighbouring vegetative cell. We estimated C_H and C_V from the pre-bleach images (e.g. Figure 3A, top left), dividing the total cell fluorescence by the estimated cytoplasmic volume (assuming a cylindrical cell). The mean value for C_V/C_H was close to 1 (1.1 ± 0.2) and thus we conclude that E_{out} and E_{in} are not significantly different: dye exchange is symmetric at heterocyst–vegetative cell junctions. This is what would be expected for a passive process with no free energy input.

We estimated E for heterocyst–vegetative cell junctions by making the simplifying approximation that concentration in the neighbouring vegetative cells remains constant. Then we expect fluorescence recovery in the heterocyst to follow a simple exponential. For a heterocyst with chains of vegetative cells on either side

$$C_H = C_0 + C_R(1 - e^{-2Et}) \quad (4)$$

where C_H is fluorescence in the heterocyst, C_0 immediately after the bleach and tending towards $(C_0 + C_R)$ after full fluorescence recovery, E is the exchange coefficient at the heterocyst–vegetative cell junctions and t is time. Similarly, for a heterocyst at the terminus of a filament

$$C_H = C_0 + C_R(1 - e^{-Et}) \quad (5)$$

These equations give a good fit to the observed recovery kinetics (Figure 3B). On average, heterocyst–vegetative cell exchange is about 13 times slower than exchange between vegetative cells in fully differentiated filaments (Table I).

In filaments grown without nitrate for 18 h there are partially developed heterocysts, which still show significant chlorophyll fluorescence (not shown). During adaptation to diazotrophic growth, molecular exchange between vegetative cells gradually becomes faster, whereas molecular exchange with the developing heterocysts becomes slower (Table I).

No molecular exchange in non-heterocystous cyanobacteria

For comparison with the data on *A. cylindrica* (Figures 1–3), we carried out similar experiments on several species of *Oscillatoria*. *Oscillatoria* are filamentous cyanobacteria that do not show heterocyst differentiation and therefore presumably have no requirement to exchange metabolites between cells (Stanier and Cohen-Bazire, 1977). One example, for *Oscillatoria terebriformis*, is shown in Figure 4. As with *A. cylindrica*, we could load calcein into the cytoplasm and bleach fluorescence within a single cell, observing rapid diffusion within the confines of the cell. However, in contrast to *A. cylindrica*, we could observe no significant fluorescence exchange between cells (Figure 4). To test whether molecular exchange in *O. terebriformis* might be induced under conditions of nutrient stress, we repeated this experiment after growth for 8 and 16 h in nitrate-free medium. We still observed no fluorescence exchange (not shown). Thus, the intercellular connections that allow calcein diffusion in *Anabaena* are absent in *Oscillatoria*. This suggests that these connections are a specific adaptation to the requirement for metabolite exchange in differentiated filaments. This conclusion is further supported by the increased rates of exchange among vegetative cells of *A. cylindrica* as the filament adapts to diazotrophic growth (Table I).

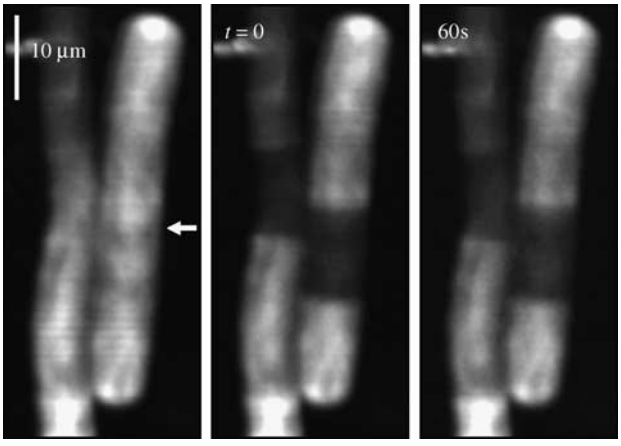

Figure 4 Calcein FRAP measurement on filaments of *Oscillatoria terebriformis*. The image at the left was recorded prior to bleaching: the arrow indicates the position of the narrow line bleach.

A quantitative model for metabolite distribution in A. cylindrica

Metabolite exchange among cells can be modelled, on the assumption that the behaviour of other small hydrophilic molecules is similar to that of calcein. This is reasonable, given that the movement of calcein appears to be due to passive diffusion, and is presumably nonspecific as calcein is not native to the cells. Other models for metabolite movement have been proposed, such as the idea that amino acids could be specifically exported from the heterocyst cytoplasm, could diffuse within a continuous periplasm and could then be specifically re-imported into the cytoplasm of vegetative cells (Flores *et al*, 2006). However, the nonspecific molecular exchange that we observe is so rapid that it must be a major route for the exchange of small hydrophilic metabolites between cells. There is no measurable calcein fluorescence in the periplasm (Figure 1), and this argues against the involvement of the periplasm in the exchange that we see. It might be possible for a molecule to be exported to the periplasm, diffuse within a continuous periplasm (Mariscal *et al*, 2007) and then be actively imported into other cells in the filament. If the active import were sufficiently rapid, this could be achieved without a high steady-state concentration in the periplasm. However, calcein is not native to the cells and therefore it is implausible that there is specific, active calcein export and import to and from the periplasm. Thus, our results are much better explained by cytoplasmic connections between cells that facilitate the rapid, passive exchange of molecules.

We used the measured exchange coefficients for fully differentiated *A. cylindrica* filaments (Table I) to model the spread along the filament of a small hydrophilic molecule synthesised in the heterocyst (Figure 5). Figure 5 shows modelling for the situation where heterocysts are separated by 10 vegetative cells. If the number of intermediate vegetative cells is increased to 20, the concentration gradient lasts longer, but even then the gradient becomes equally flat within about 8 min of the onset of 'metabolite synthesis' (not shown). The rapid exchange between vegetative cells means that the concentration of the molecule could be almost independent of position in the filament (Figure 5). Thus, rapid molecular exchange could ensure an even distribution

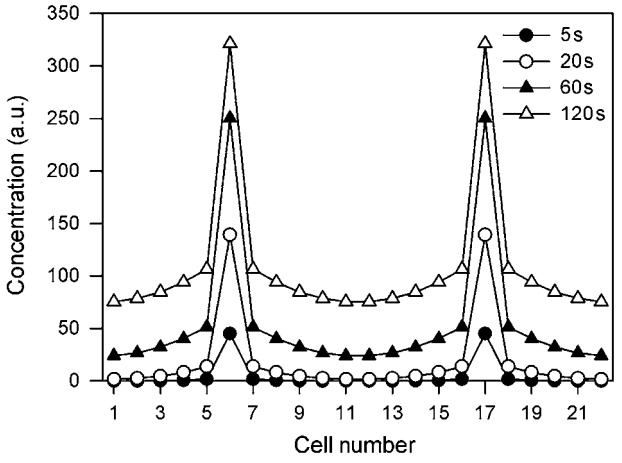

Figure 5 Modelling the equilibration of a molecule synthesised in the heterocyst. The model represents a 22-cell filament. Cells 6 and 17 are heterocysts and the remainder are vegetative cells. The heterocysts begin to synthesise a molecule at time zero, and then continue to produce it at a constant rate. Spread of the molecule is modelled assuming $E = 0.022\,s^{-1}$ (heterocyst–vegetative cell exchange) and $0.29\,s^{-1}$ (exchange between vegetative cells) (Table I). The predicted relative concentration in each cell is shown for various time points.

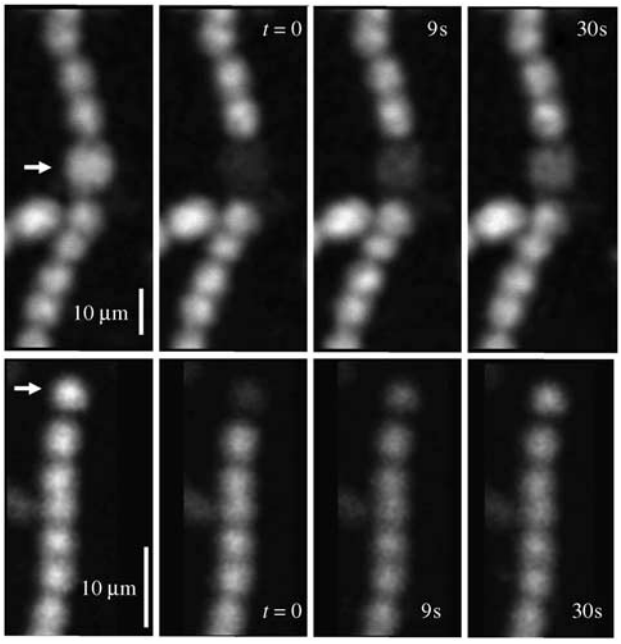

Figure 6 FRAP measurements of calcein exchange between vegetative cells and heterocysts in *Anabaena variabilis*. Top: wild type. Bottom: Δ*cph*A. In both cases, calcein fluorescence in a heterocyst was bleached (position of bleach indicated by the arrows). Note that the heterocyst in Δ*cph*A is at the end of the filament: this is typical for this mutant.

of metabolites among vegetative cells. However, note that the true situation for an amino acid (for example) will be more complex because of metabolism by the vegetative cells. Data on rates of metabolite production and utilisation will need to be incorporated into the model to give more realistic picture of metabolite distribution in the filament.

Cyanophycin 'plugs' reduce the rate of molecular influx into heterocysts

Heterocysts maintain a microaerobic environment for nitrogen fixation, necessary because nitrogenase is inactivated by oxygen (Wolk *et al*, 1994). Heterocysts have an additional surrounding glycolipid 'laminated' layer that acts as a barrier to the influx of gases, including oxygen, from the external medium. Where the heterocyst adjoins the neighbouring vegetative cell, the laminated layer is greatly thickened, reducing the area of contact between the cells to a narrow 'neck' (Lang and Fay, 1971; Flores *et al*, 2006), through which intercellular communication must occur (Walsby, 2007). Our results suggest that molecular exchange with vegetative cells must lead to significant oxygen influx into heterocysts. Oxygen will be produced by photosynthetic electron transport in the vegetative cells. It is a smaller molecule than calcein and must diffuse at least as fast. The gas exchange problem in filamentous cyanobacteria is thoroughly discussed by Walsby (2007). Heterocysts show increased oxidase activity (Wolk *et al*, 1994), as a result of increased expression of genes encoding terminal respiratory oxidases (Valladares *et al*, 2003, 2007). The lower rate of molecular exchange between vegetative cells and heterocysts (Table I) may serve to keep oxygen influx into the heterocyst slow enough to be countered by oxidase activity.

Several factors may contribute to the slower molecular exchange with heterocysts. The narrow 'neck' reduces the area of the cell–cell interface (Lang and Fay, 1971; Flores *et al*, 2006; Walsby, 2007). The 'microplasmodesmata' observed by freeze-fracture electron microscopy may well be the channels through which molecular exchange occurs. On average, there are about 50 microplasmodesmata at the heterocyst–vegetative cell interface compared with 200–300 at vegetative–vegetative cell interfaces (Giddings and Staehelin, 1978). A further possible factor is the presence of 'plugs' or polar nodules of cyanophycin in heterocysts. These plugs appear to block the connections between the heterocysts and their vegetative neighbours, as can be observed in electron micrographs (Ziegler *et al*, 2001). To test this possibility, we exploited the availability of a mutant of *Anabaena variabilis* lacking cyanophycin synthase (Δ*cphA*). This mutant does not form the polar nodules. It is still capable of heterocyst differentiation and diazotrophic growth, although diazotrophic growth at high light intensities is somewhat slower than in the wild type (Ziegler *et al*, 2001).

We grew *A. variabilis* diazotrophically to induce heterocyst differentiation, and then loaded filaments of the wild type and Δ*cphA* with calcein as described above for *A. cylindrica*. In our hands, nearly all the heterocysts in Δ*cphA* were at the ends of filaments. However, we can be sure that these terminal heterocysts are not 'leaky' as calcein was retained in the filament as well in Δ*cphA* as in all the other strains we used. We performed FRAP measurements bleaching the heterocyst, and determined the exchange coefficient for vegetative cell–heterocyst exchange. The equations used distinguish between terminal and non-terminal heterocysts, as non-terminal heterocysts exchange with vegetative cells on both sides (see Equations (4) and (5)). We found that exchange of calcein between vegetative cells and heterocysts was significantly faster for Δ*cphA* than for the wild type (Figure 6). For wild-type cells, we obtained a mean value for E of $0.020 \pm 0.016\,s^{-1}$, comparable to *A. cylindrica* (Table I). For Δ*cphA*, we obtained a mean value of

$0.067 \pm 0.039\ s^{-1}$. A *t*-test indicates that the difference is highly significant ($P = 0.002$). This strongly suggests that the cyanophycin plugs reduce the rate of molecular exchange between vegetative cells and heterocysts.

FraG as a candidate for the channel-forming protein

The studies described so far strongly suggest that there is a specific structure that forms channels between cells in *Anabaena* that allow small molecules to diffuse from cytoplasm to cytoplasm. Intercellular molecular exchange almost certainly depends on specific protein machinery, as it is absent in *Oscillatoria* (Figure 4) and in *A. cylindrica* it is upregulated during adaptation to diazotrophic growth (Table I). The channels allow rapid diffusion of the 623-Da calcein molecule (and presumably any smaller hydrophilic molecules). However, they do not allow the diffusion of GFP, a 27-kDa protein. This is clear, as cytoplasmic GFP does not spread from cell to cell in *Anabaena* filaments (Yoon and Golden, 1998; Mariscal *et al*, 2007). This gives only a very crude indication of the size discrimination of the channels, but so far they appear to show some of the functional properties of the gap junctions of animal cells, which allow the free diffusion of molecules up to about 1 kDa, but not proteins or nucleic acids (Söhl *et al*, 2005).

Flores *et al* (2007) recently used a range of molecular approaches to characterise a protein that they named SepJ, but which had also been named FraG (Nayar *et al*, 2007). We will refer to it here as FraG. FraG is the product of the open reading frame (ORF) *alr2338* in *Anabaena* sp. PCC7120. This protein has a number of features that suggest it as a strong candidate for the channel former. It has a 340-residue C-terminal domain, which is predicted to be membrane integral and shows homology to proteins in the bacterial drug/metabolite exporter (DME) family (Flores *et al*, 2007). This could form the channel allowing hydrophilic molecules to traverse the plasma membrane. It has a large extracytoplasmic portion (with extensin-like and coiled-coil domains) (Flores *et al*, 2007) that could be involved in spanning the cell wall and bridging the gap between adjacent cells in the filament. GFP tagging shows that FraG in *Anabaena* 7120 is localised in the plasma membrane at the cell–cell interface, and it is expressed in heterocysts as well as vegetative cells (Flores *et al*, 2007). Although substantial levels of FraG are present in cells grown in the presence of combined nitrogen, *fraG* mRNA levels increase during adaptation to diazotrophic growth, and *fraG* null mutants (Δ*fraG*) are incapable of full heterocyst differentiation and diazotrophic growth (Flores *et al*, 2007; Nayar *et al*, 2007).

BLAST searches (not shown) show that *fraG* is conserved in the other filamentous, heterocyst-forming cyanobacteria for which complete genome sequences are available (*Nostoc punctiforme*, *A. variabilis* and *Nodularia spumigena*). We could find no significant full-length homologs in any other organism. However, there are truncated homologs in the filamentous, non-heterocyst-forming cyanobacteria *Trichodesmium erythraeum* and *Lyngbya* sp. and the unicellular cyanobacterium *Synechocystis* sp. PCC6803. The *Trichodesmium* and *Lyngbya* homologs lack the extensin-like domain, and the *Synechocystis* homolog lacks both this domain and the coiled-coil domain.

To test the possibility that FraG is involved in intercellular molecular exchange, we performed calcein FRAP measurements on *Anabaena* 7120 wild type and Δ*fraG*. Exchange coefficients are summarised in Table II. We found that for wild-type *Anabaena* 7120 grown on nitrate, molecular exchange between vegetative cells is relatively slow on average, and is very variable from filament to filament (Table II). However, as cells adapt to diazotrophic growth, there is a considerable increase in the rate of cell–cell exchange, by a factor more than 10 in fully differentiated filaments (Table II). Qualitatively, this is the same effect as that seen in *A. cylindrica* (Table I), but the induction of intercellular exchange is more dramatic in *Anabaena* 7120. We found that rates of molecular exchange in nitrate-grown filaments of Δ*fraG* are extremely low (Table II). Comparison with nitrate-grown wild type shows that exchange in Δ*fraG* is significantly slower, despite the low rate of exchange in wild-type cells under these conditions (Table II). For a further comparison between wild type and Δ*fraG*, we compared rates of exchange after 16 h of nitrate deprivation. This is long enough for the induction of significantly faster exchange in the wild type (Table II), but not long enough to lead to cell death or complete filament fragmentation in Δ*fraG* (Flores *et al*, 2007; Nayar *et al*, 2007). An unexpected problem was that uptake of calcein-AM by Δ*fraG* cells after 16 h of nitrate deprivation was very poor (data not shown), presumably due to unknown changes in cell surface properties. So to compare wild type with Δ*fraG*, we incubated nitrate-grown filaments of the two strains with calcein-AM before washing and growing for 16 h in nitrate-free medium. The dye was very well retained in the filaments and we were then able to perform FRAP measurements. Typical examples are shown in Figure 7, with mean exchange coefficients in Table II. Δ*fraG* filaments are typically very short (e.g. Figure 7) due to their fragility (Flores *et al*, 2007; Nayar *et al*, 2007). In Δ*fraG*, as in all the other strains we examined, there is rapid diffusion of calcein within the cytoplasm of the bleached

Table II Cell–cell exchange coefficients for calcein in filaments of *Anabaena* sp. PCC7120

Measurement	Mean exchange coefficient (s^{-1}) ($\pm$s.d.)
1. Wild-type vegetative cells in nitrate-grown filaments	0.021 ± 0.011
2. Wild-type vegetative cells after 16 h of nitrate deprivation	0.057 ± 0.039
3. Wild-type vegetative cells after 96 h of nitrate deprivation	0.28 ± 0.12
4. Wild-type (vegetative cells to heterocysts) after 96 h of nitrate deprivation	0.035 ± 0.012
5. Δ*fraG* vegetative cells in nitrate-grown filaments	0.007 ± 0.008
6. Δ*fraG* vegetative cells after 16 h of nitrate deprivation	0.002 ± 0.002

t-Tests indicate that *E* is significantly different in (1) and (2) ($P = 0.008$); (2) and (3) ($P = 0.00002$); (3) and (4) ($P = 0.0015$); (1) and (5) ($P = 0.004$); (2) and (6) ($P = 0.004$); (4) and (5) ($P = 0.00008$).

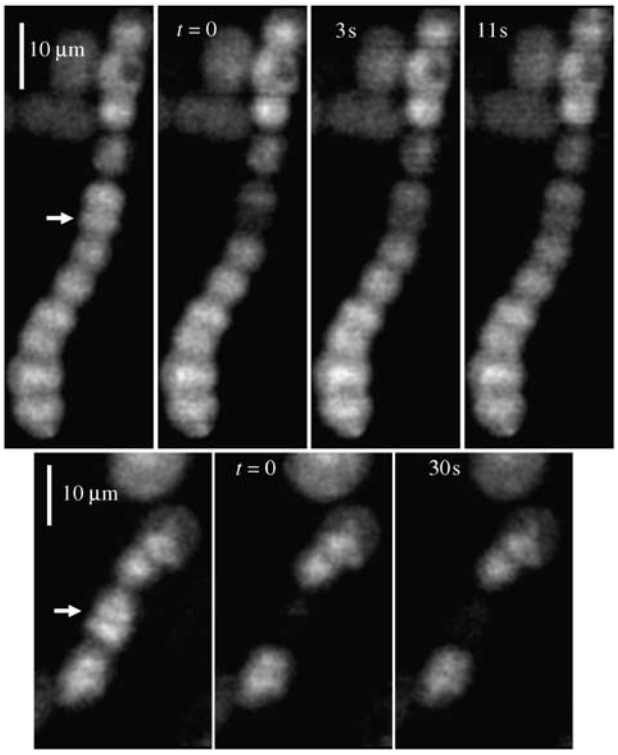

Figure 7 Calcein FRAP measurements on vegetative cells of *Anabaena* 7120, grown for 16 h in nitrate-free medium. The sequence at the top is for wild type, and the sequence underneath is for Δ*fraG*. The arrows show the position of the line bleach. In both cases, we show sequences where the measured exchange coefficient is close to the mean (Table II).

cell (Figure 7). However, exchange of calcein between cells is negligible in Δ*fraG* (exchange about 30 times slower on average than for the wild type under the same conditions, $P = 0.004$) (Figure 7 and Table II).

It is clear that Δ*fraG* is perturbed in its ability to acclimate to nitrate deprivation (Flores *et al*, 2007). Therefore, we cannot exclude an indirect explanation for the result shown in Figure 7. It is possible that the lack of intercellular exchange in Δ*fraG* after 16 h of nitrate deprivation is an indirect consequence of its inability to acclimate to these conditions. It is also possible that impairment in exchange results from altered cohesiveness in filaments of Δ*fraG*. However, in view of the significant difference between wild type and Δ*fraG* even when grown on nitrate (Table II), and the very suggestive features of FraG discussed above, we think it much more likely that FraG is part of the molecular machinery required for intercellular molecular exchange. This would explain many aspects of the Δ*fraG* phenotype, including the inability of the mutant to grow diazotrophically and differentiate heterocysts. The intercellular channels may incorporate other proteins as well. The Fra proteins are a set of proteins identified on genetic grounds as being important for filament integrity under diazotrophic conditions (Buikema and Haselkorn, 1991; Bauer *et al*, 1995). Any of these might be candidates for involvement in intercellular channel function. Note however that an electron micrograph clearly shows the putative intercellular connections in a *fraC* null mutant (Bauer *et al*, 1995), suggesting that FraC is not a major structural component of the channels. The domain structure of FraG (discussed above) suggests that it may well be the major structural component of the channels. Consistent with this, electron micrographs of cell junctions in Δ*fraG* (e.g. Flores *et al*, 2007 and further unpublished examples) show no evidence of the putative intercellular channels. However, these are not always resolved in the wild type.

Formation and regulation of intercellular channels

Our results show significant upregulation of intercellular molecular exchange between vegetative cells upon acclimation to diazotrophic growth (Tables I and II). However, electron microscopy suggests that the number of channels between vegetative cells does not increase significantly upon acclimation to diazotrophic growth. In *A. cylindrica*, there are about 175–250 microplasmodesmata at each junction between vegetative cells in nitrate-grown filaments (Giddings and Staehelin, 1981) and about 200–300 in filaments growing diazotrophically (Giddings and Staehelin, 1978). Consistent with this, GFP tagging of FraG in *Anabaena* 7120 shows significant FraG at cell junctions in nitrate-grown filaments (Flores *et al*, 2007), even though rates of molecular exchange are very low under these conditions (Table II). This suggests an unknown regulatory mechanism that controls the activity of the channels, allowing faster molecular exchange among vegetative cells as the filament adapts to diazotrophic growth. Such a mechanism is probably necessary because the presence of the cell wall makes it hard to form the channels *de novo* at pre-existing cell junctions. We suppose that channels are formed by FraG subunits (possibly together with other proteins) located in the plasma membranes of the two adjacent cells. To form a complete channel, the subunits in the two membranes would have to align and link together across the intercellular gap. In animal gap junctions, this is straightforward because connexin subunits in the two membranes can diffuse laterally until they locate each other (Söhl *et al*, 2005). By contrast, the cyanobacterial half-channels must be locked in place, because they must penetrate through the cell wall, a rigid polymer. It may therefore only be possible to form the channels as the cell divides, before cell wall formation inhibits lateral diffusion. Indeed, electron microscopy shows that microplasmodesmata form during cytokinesis (Giddings and Staehelin, 1978) and GFP tagging shows that FraG starts to locate at the site of cell division at a very early stage in cytokinesis (Flores *et al*, 2007). This would explain the necessity for constitutive formation of the channels, with regulation of their activity. Clearly a system for metabolite distribution based on sequential exchange through the chain of vegetative cells can only operate successfully if all the cell junctions are permeable to metabolites, including any cell junctions that were formed prior to the switch to diazotrophic growth.

Summary of conclusions

1. In *Anabaena* filaments, there is rapid exchange of calcein, a small (623 Da) hydrophilic molecule, between the cytoplasms of neighbouring cells. Molecular exchange appears to be a nonspecific, non-directional and passive process, driven by random diffusion of the molecule.
2. If calcein, a non-indigenous molecule, can exchange rapidly between cells, it is almost certain that other small, hydrophilic molecules in the cytoplasm will behave in the

same way. Such molecules would include sugars and some amino acids, which must be exchanged between heterocysts and vegetative cells in differentiated filaments.
3. Molecular exchange must require a specific cellular machinery, as in *Anabaena* it is upregulated in response to nitrate deprivation (Tables I and II), and furthermore it is absent in the non-heterocyst-forming *Oscillatoria* (Figure 4) and in an *Anabaena* mutant (Figure 7).
4. Molecular exchange between heterocysts and vegetative cells is considerably slower than exchange among vegetative cells (Tables I and II). This is probably an adaptation to reduce the rate of oxygen influx into the heterocyst cytoplasm. The formation of cyanophycin 'plugs' or polar nodules in heterocysts is one of the factors that reduces the rate of molecular exchange between heterocysts and vegetative cells (Figure 6).
5. The dynamics of molecular exchange in *Anabaena* filaments could lead to a rather uniform distribution of metabolites among vegetative cells (Figure 5), though this will also depend on the rates of metabolite production and utilisation.
6. FraG (or SepJ), the product of ORF *alr2338* in *Anabaena* 7120, has many of the features that would be expected of a protein forming the channels required for intercellular molecular exchange. Consistent with this idea, we found negligible rates of molecular exchange in a *fraG* null mutant (Table II and Figure 7).
7. FraG is probably an essential component of structures that form intercellular channels linking the cytoplasms of cells in *Anabaena* filaments. The channels allow the non-selective diffusion of small molecules. To our knowledge, this is the first demonstration of such a mode of cell communication in a prokaryote.

Materials and methods

Strains and culture conditions

The species used were *A. cylindrica* (Pasteur Culture Collection sp. PCC7122), *A. variabilis* (ATCC 29413), *Anabaena* (or *Nostoc*) sp. PCC7120, and *O. terebriformis*. All species were grown in liquid BG11 medium (Castenholz, 1988) supplemented with 10 mM $NaHCO_3$. Growth medium for *A. variabilis* Δ*cphA* (Ziegler *et al*, 2001) was supplemented with kanamycin (50 μg ml^{-1}) and growth medium for *Anabaena* 7120 Δ*fraG* (strain SR2787a) (Flores *et al*, 2007) was supplemented with erythromycin (5 μg ml^{-1}). Cultures were grown in 250 ml conical flasks in an orbital incubator at 30°C, under constant white light at 15 μE m^{-2} s^{-1}. Heterocyst differentiation was induced by growth for up to 96 h in nitrate-free BG11 medium, in which the ferric ammonium citrate (Castenholz, 1988) was also replaced by ferric citrate. The cells were first harvested by gentle centrifugation and washed several times in nitrate-free medium.

Labelling with fluorescent dyes

Calcein-AM and BODIPY® FL-C_{12} were obtained from Invitrogen (Haugland, 2005). For calcein staining, 0.5 ml of cell culture was harvested by gentle centrifugation, washed several times and resuspended in 0.5 ml fresh growth medium, and then mixed with 10 μl of calcein-AM (1 mg/ml in dimethylsulphoxide). The suspension was incubated in the dark at 30°C for 90 min, and cells were then harvested and washed three times in fresh, dye-free growth medium. The suspension was then incubated in the dark for a further 90 min before imaging, except for *Anabaena* 7120 (wild type and Δ*fraG*) after 16 h of nitrate deprivation. In this case, cells were grown in nitrate, loaded with calcein, washed in dye-free, nitrate-free medium and then grown in the light for 16 h before measurement. BODIPY staining followed the same protocol as for calcein-AM, except that cells were mixed with 2.5 μl of BODIPY® FL-C_{12} (1 mM in dimethylsulphoxide).

Confocal microscopy and FRAP

Cell suspensions were spotted onto agar plates (1.5% Bacto-Agar with growth medium) and the excess liquid was allowed to dry or absorb. Small blocks of agar with cells were then cut out and placed in a custom-built temperature-controlled sample holder with a glass cover slip on top (Mullineaux and Sarcina, 2002). All measurements were carried out at 30°C. Cells were imaged with a laser-scanning confocal microscope (Nikon PCM2000) using a ×60 oil-immersion objective and the 488 nm line of a 100 mW argon laser (Spectra-Physics) as the excitation source. Chlorophyll fluorescence and dye fluorescence were imaged simultaneously, chlorophyll fluorescence being defined by a Schott RG665 red-glass filter, and dye fluorescence by an interference band-pass filter transmitting between 500 and 527 nm. For imaging, a 20 μm confocal pinhole was used, giving a point spread in the *Z*-direction of about 1.3 μm (full width at half-maximum). For FRAP, a 50 μm pinhole was used, increasing the point spread in the *Z*-direction to about 2.0 μm. An initial image was recorded, and the bleach was then carried out by switching the microscope to X-scanning mode, increasing the laser intensity by a factor of 32 by removing neutral density filters, and scanning a line across one cell for 1–2 s. The laser intensity was then reduced again, the microscope was switched back to XY-imaging mode and a sequence of images recorded typically at 3-s intervals.

FRAP data analysis and modelling

Total fluorescence in each cell in the filament, at each time point, was quantified using Image Pro Plus 6.2 software (Media Cybernetic Inc.). Relative fluorescence profiles were obtained by dividing the fluorescence in each cell by the value prior to the bleach. To estimate *E* in vegetative cells, the first post-bleach profile was taken, and the evolution of the fluorescence profile was predicted using an iterative computer routine running in SigmaPlot 10.0 (Jandel Scientific). Incremental concentration changes were calculated according to Equation (2). The initial assumed value for *E* was always 0.01 s^{-1} and the time increment was 1 ms. The predicted fluorescence recovery of the bleached cell was then fitted to the experimental recovery curve by adjusting the time axis, to obtain an estimate of *E*. *E* for heterocyst–vegetative cell exchange was estimated by curve fitting according to Equation (4) (for heterocysts in the middle of filaments) or Equation (5) (for terminal heterocysts). All curve fitting used Sigmaplot 10.0. Modelling of metabolite spread in filaments used an iterative routine running in SigmaPlot as described above, with modifications to the programme to allow different values of *E* for the heterocyst and vegetative cells, and continuous production of the metabolite in the heterocyst.

Acknowledgements

We thank Wolfgang Lockau (Humboldt-Universität Berlin) for the gift of *A. variabilis* Δ*cph*A and Richard Castenholz (University of Oregon) for the gift of *O. terebriformis*. We acknowledge earlier preliminary work carried out in CWM's laboratory by Rasmi Pillai and Mary Sarcina. The project used equipment purchased with grants to CWM from the Wellcome Trust and Biotechnology and Biological Sciences Research Council. Financial support to EF from Ministerio de Educación y Ciencia (Spain), grant number BFU2005-07672, is acknowledged.

References

Bauer CC, Buikema WJ, Black K, Haselkorn R (1995) A short-filament mutant of *Anabaena* sp. strain PCC 7120 that fragments in nitrogen-deficient medium. *J Bacteriol* **177:** 1520–1526

Buikema WJ, Haselkorn R (1991) Isolation and complementation of nitrogen fixation mutants of the cyanobacterium *Anabaena* sp. strain PCC 7120. *J Bacteriol* **173:** 1879–1885

Castenholz RW (1988) Culturing methods for cyanobacteria. In *Methods in Enzymology Vol. 167. Cyanobacteria*, Packer L, Glazer AN (eds), pp 68–93. San Diego: Academic Press

Flores E, Herrero A, Wolk CP, Maldener I (2006) Is the periplasm continuous in filamentous multicellular cyanobacteria? *Trends Microbiol* **14:** 439–443

Flores E, Pernil R, Muro-Pastor AM, Mariscal V, Maldener I, Lechno-Yossef S, Fan Q, Wolk CP, Herrero A (2007) Septum-localized protein required for filament integrity and diazotrophy in the heterocyst-forming cyanobacterium *Anabaena* sp. strain PCC 7120. *J Bacteriol* **189:** 3884–3890

Giddings TH, Staehelin LA (1978) Plasma membrane architecture of *Anabaena cylindrica*: occurrence of microplasmodesmata and changes associated with heterocyst development and the cell cycle. *Eur J Cell Biol* **16:** 235–249

Giddings TH, Staehelin LA (1981) Observation of microplasmodesmata in both heterocyst-forming and non-heterocyst forming filamentous cyanobacteria by freeze-fracture electron microscopy. *Arch Microbiol* **129:** 295–298

Golden JW, Yoon HS (2003) Heterocyst development in *Anabaena*. *Curr Opin Microbiol* **6:** 557–563

Haugland RP (2005) *The Handbook—a Guidebook to Fluorescent Probes and Labelling Technologies*. Carlsbad, CA, USA: Invitrogen Corp.

Komenda J, Barker M, Kuvikova S, De Vries R, Mullineaux CW, Tichy M, Nixon PJ (2006) The FtsH protease, slr0228, is important for quality control of the thylakoid membrane of *Synechocystis* PCC6803. *J Biol Chem* **281:** 1145–1151

Lang N, Fay P (1971) The heterocysts of blue-green algae. II. Details of ultrastructure. *Proc R Soc Lond B* **178:** 193–203

Lucas WJ, Lee J-Y (2004) Plasmodesmata as a supracellular control network in plants. *Nat Rev Mol Cell Biol* **5:** 712–726

Mariscal V, Herrero A, Flores E (2007) Continuous periplasm in a filamentous, heterocyst-forming cyanobacterium. *Mol Microbiol* **65:** 1139–1145

Mullineaux CW, Nenninger A, Ray N, Robinson C (2006) Diffusion of green fluorescent protein in three cell environments in *Escherichia coli*. *J Bacteriol* **188:** 3442–3448

Mullineaux CW, Sarcina M (2002) Probing the dynamics of photosynthetic membranes with fluorescence recovery after photobleaching. *Trends Plant Sci* **7:** 237–240

Nayar AS, Yamaura H, Rajagopalan R, Risser DD, Callahan SM (2007) FraG is necessary for filament integrity and heterocyst maturation in the cyanobacterium *Anabaena* sp. strain PCC7120. *Microbiology* **153:** 601–607

Sarcina M, Murata N, Tobin MJ, Mullineaux CW (2003) Lipid diffusion in the thylakoid membranes of the cyanobacterium *Synechococcus* sp.: effect of fatty acid desaturation. *FEBS Lett* **553:** 295–298

Söhl G, Maxeiner S, Willecker K (2005) Expression and functions of neuronal gap junctions. *Nat Rev Neurosci* **6:** 191–200

Spence E, Sarcina M, Ray N, Møller SG, Mullineaux CW, Robinson C (2003) Membrane-specific targeting of green fluorescent protein by the Tat pathway in the cyanobacterium *Synechocystis* PCC6803. *Mol Microbiol* **48:** 1481–1489

Stanier RY, Cohen-Bazire G (1977) Phototrophic prokaryotes: the cyanobacteria. *Ann Rev Microbiol* **31:** 225–274

Valladares A, Herrero A, Pils D, Schmetterer G, Flores E (2003) Cytochrome *c* oxidase genes required for nitrogenase activity and diazotrophic growth in *Anabaena* sp PCC 7120. *Mol Microbiol* **47:** 1239–1249

Valladares A, Maldener I, Muro-Pastor AM, Flores E, Herrero A (2007) Heterocyst development and diazotrophic metabolism in terminal respiratory oxidase mutants of the cyanobacterium *Anabaena* sp strain PCC 7120. *J Bacteriol* **189:** 4425–4430

Walsby AE (2007) Cyanobacterial heterocysts: terminal pores proposed as sites of gas exchange. *Trends Microbiol* **15:** 340–348

Wolk CP (1991) Genetic analysis of cyanobacterial development. *Curr Opin Genet Dev* **1:** 336–341

Wolk CP, Ernst A, Elhai J (1994) Heterocyst metabolism and development. In *Molecular Biology of Cyanobacteria. Advances in Photosynthesis and Respiration*, Bryant DA (ed), Vol. 1, pp 769–823. Dordrecht: Springer

Xu X, Elhai J, Wolk CP (2008) Transcriptional and developmental responses by *Anabaena* to deprivation of fixed nitrogen. In *The Cyanobacteria. Molecular Biology, Genomics and Evolution*, Herrero A, Flores E (eds), pp 383–422. Norfolk: Caister Academic Press

Yoon H-S, Golden JW (1998) Heterocyst pattern formation controlled by a diffusible peptide. *Science* **282:** 935–938

Zhang C-C, Laurent S, Sakr S, Peng L, Bédu S (2006) Heterocyst differentiation and pattern formation in cyanobacteria: a chorus of signals. *Mol Microbiol* **59:** 367–375

Ziegler K, Stephan DP, Pistorius EK, Ruppel HG, Lockau W (2001) A mutant of the cyanobacterium *Anabaena variabilis* ATCC 29413 lacking cyanophycin synthetase: growth properties and ultrastructural aspects. *FEMS Microbiol Lett* **196:** 13–18

